Electronic Structure of the Superatom: A Quasiatomic System Based on a Semiconductor Heterostructure

Takeshi Inoshita, Shuhei Ohnishi, and Atsushi Oshiyama

Fundamental Research Laboratories, NEC Corporation, Miyamae-ku, Kawasaki 213, Japan

(Received 28 July 1986)

The electronic structure of the superatom, a recently proposed mesoscopic system made of a spherical semiconductor heterostructure, is investigated by a self-consistent local-density-functional calculation. Numerical results on AlGaAs-GaAs superatoms reveal that the atomic-orbital picture can be successfully applied and that the ground-state configuration is stable at $T \sim 1$ K. The electronic level structure, however, is quite distinct from that of ordinary atoms because of the absence of the $1/r$ singularity in the potential.

PACS numbers: 71.55.−i, 31.20.Gm, 73.40.Lq

Recent innovations in microfabricration technology have made it possible to realize various quantum structures and are now opening the gate to a new realm of physics called mesoscopic physics.[1,2] Although many of the efforts thus far have been directed to two- and one-dimensional structures, the possibility of fabricating a quasiatomic system with use of a semiconductor heterostructure was pointed out by Watanabe on the basis of the current status and the future prospect of microfabrication technology.[3,4] This novel structure was named "superatom."

While the superatom is considered useful from the applications point of view (use of a superatom array for functional devices has been suggested),[4] we can also expect it to have unique physical properties both in itself and in the form of superatom "molecules" or "crystals." The purpose of the present work is to clarify the general features of the electronic structure of the superatom through a fully quantum mechanical self-consistent calculation and hence to provide a basis for the understanding of this novel system.

A superatom is a semiconductor heterostructure made of a spherical core, modulation-doped with a controlled number (z) of donors, and a surrounding impurity-free matrix with larger electron affinity (Fig. 1). If the conduction-band offset at the interface is sufficiently large, all the donors in the core are ionized and produce a nearly centrosymmetric Coulomb potential outside the core, which, in turn, binds the z electrons released from the donors. (Since the matrix is assumed to be impurity-free, the Fermi level is determined solely by the z electrons and is always adjusted so that all the electrons are bound at $T=0$.) Watanabe speculated that, if the core radius is sufficiently small, the electronic system can be described as a quasiatom with well-defined atomic orbitals, z being the "atomic number." Promising candidate materials for the superatom include $Al_xGa_{1-x}As$(core)-GaAs(matrix), SiO_2(core)-Si(matrix), and InP(core)-$In_{0.53}Ga_{0.47}As$(matrix). In the following, we report the results of our calculation on $Al_{0.35}Ga_{0.65}As$-GaAs.

In calculating the electronic structure of the superatom, we follow the standard self-consistent nonrelativistic treatment for the atom[5] and assume the potential to be spherically symmetric. An eigenfunction for Schrödinger's equation can be separated into radial and angular parts as $[X(r)/r]Y_{lm}(\theta\phi)$ and the radial part satisfies (in atomic units)

$$\left[-\frac{1}{2m^*}\frac{d^2}{dr^2}+\frac{l(l+1)}{2m^*r^2}+V(r)\right]X(r)=EX(r), \tag{1}$$

where the effective mass m^* is taken to be position dependent and is set equal to the conduction-band effective mass of $Al_{0.35}Ga_{0.65}As$ or GaAs depending on whether r is inside or outside of the core.[6] For the potential $V(r)$, we take

$$V(r)=E_{\text{offset}}\Theta(R_c-r)+V_{\text{core}}(r)+V_{\text{H}}(r)+V_{\text{xc}}(r).$$

Here the first term takes care of the band offset, $\Theta(r)$ being the step function. V_{core} is the potential due to the ionized donors and is approximated by the potential for a uniformly charged sphere, i.e., $ze/\varepsilon_m r$ outside the core and $ze/\varepsilon_m R_c + ze(R_c^2-r^2)/2\varepsilon_c R_c^3$ inside (ε_m and ε_c are the dielectric constants of the matrix and core, respectively, and R_c the core radius). The Hartree potential V_{H} due to the electrons is numerically calculated as a sum of one-dimensional integrals of the spherical charge

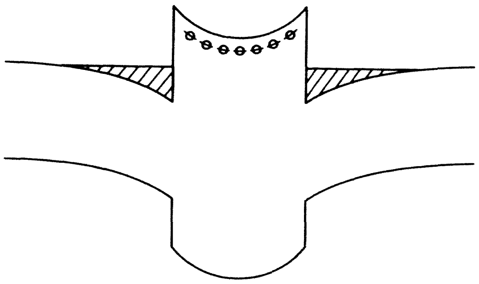

FIG. 1. Conduction- and valence-band edge diagram for a superatom. Coulomb field due to ionized donors (open circles) binds electrons (shaded areas) to form a quasiatomic electronic system.

density. As for the exchange-correlation part V_{xc}, we use an analytic expression[7] for the local-density-functional potential by Ceperley and Alder obtained by a Monte Carlo method.[8] Inclusion of m^* and ε in the Ceperley-Alder potential $U_{xc}(r_s)$ is carried out by the relation $V_{xc}(r) = (m^*/\varepsilon^2)U_{xc}[(m^*/\varepsilon)r_s(r)]$.[9] The contribution of the image force has been known to be of minor importance[10] and was therefore neglected. The parameters we use are $\varepsilon = 12.9$ and $m^* = 0.067m_0$ for GaAs, $\varepsilon = 11.8$ and $m^* = 0.082m_0$ for $\mathrm{Al_{0.35}Ga_{0.65}As}$, and $E_{\mathrm{offset}} = 0.29$ eV.

Figure 2 shows the self-consistently obtained potential, orbital energies, and the radial wave functions $X_{nl}(r)/r$ for the ground-state configuration $(1s^2 2p^6 3d^{10} 2s^2)$ of the superatom with $z = 20$ and $R_c = 120$ Å. The most striking feature is the level sequence $1s, 2p, 3d, \ldots$, which is in marked contrast with the familiar atomic sequence $1s, 2s, 2p, 3s, 3p$, etc. Before going further into it, let us remind ourselves that Schrödinger's equations [Eq. (1)] for different l are independent, and the solutions for each l are conventionally numbered in increasing magnitude of energy by the integer n starting from $n = l+1$. Also, since the centrifugal potential in Eq. (1) increases with l, the eigenvalues satisfy $E_{1s} < E_{2p} < E_{3d} < \ldots$, $E_{2s} < E_{3p} < E_{4d} < \ldots$, etc. Now ordinary atoms are characterized by the singularly deep Coulomb potential at $r = 0$ with the consequence that low angular momentum states, having larger amplitude around $r = 0$, are favored. Hence $2s$ comes between $1s$ and $2p$, $3s$ and $3p$ between $2p$ and $3d$, and so on. Superatoms, on the other hand, lack such a singularity, and therefore states with fewer radial nodes are favored. Actually we found out that no-radial-node states $(1s, 2p, 3d, \ldots)$ dominate the superatom electronic structure for a wide range of system parameters. Of course, in the limit $R_c \to 0$ or $z \to \infty$, we should recover the ordinary atomic sequence, but in reality this situation is hardly realized, because R_c and z are bounded by the conditions that (1) the donor concentration should be less than the donor solubility limit ($\sim 10^{19}$ cm^{-3}), and (2) the donor levels should be higher in energy than the outermost occupied orbital in order for all the donors to be ionized, and, therefore, for the superatom concept to be valid. [As R_c is reduced or z is increased, $V(r \approx 0)$ is lowered, eventually resulting in a violation of this latter condition.] The level sequence for the superatom $1s, 2p, 3d, \ldots$ bears a close similarity to that of alkali-metal fine particles.[11] This is somewhat surprising because, although the lack of a singularity in the potential is common to both, the detailed potential forms are quite distinct, since the band offset is absent in a fine particle.

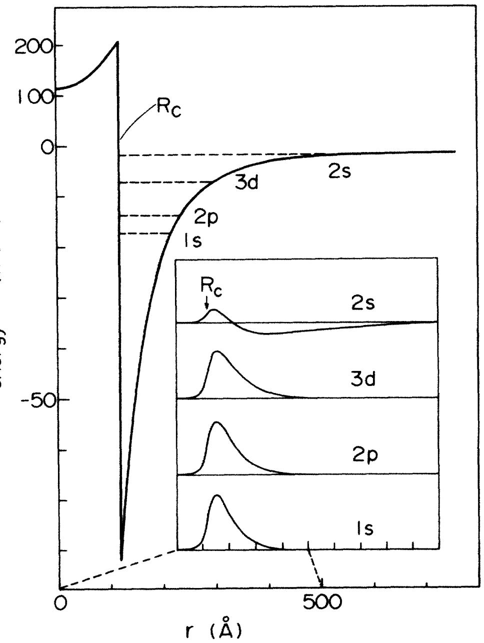

FIG. 2. Self-consistently obtained potential $V(r)$ (solid line) and orbital energies (broken line) for an $\mathrm{Al_{0.35}Ga_{0.65}As}$-GaAs superatom with $z = 20$ and $R_c = 120$ Å. The zero of energy is equal to $V(\infty)$. Note the difference in the scales in the ordinate for positive and negative regions. Inset: The normalized radial wave function $X_{nl}(r)/r$.

From Fig. 2, it is also seen that the highest occupied orbital $2s$ is well extended, and the "superatomic radius" as defined by the maximum of the radial wave function $X_{2s}(r)/r$ is 355 Å$\cong 3R_c$. This confirms the validity of the atomic-orbital picture of the superatomic electronic structure conjectured in Ref. 1. This is a significant result which indicates the feasibility of forming a superatom "molecules" or "crystals" (i.e., itinerant-electronic systems) by arrangement of superatoms in a suitable manner.

Figure 3 presents the atomic number (z) dependence of the ground-state orbital energies, the ground-state configuration being determined by comparison of the total energy calculated for several possible configurations. Up to $z = 18$, the electrons fill consecutively the no-node sequence $1s$, $2p$, and $3d$, and closed-shell configurations are reached at $z = 2$, 8, and 18. An interesting situation arises when the electrons start filling the first one-node state $2s$. (See also Table I.) As z goes beyond 19, the electrons first fill the $2s$ states and then set out to fill the $4f$ states, but with a further increase of z, one of the $2s$ electrons is transferred to $4f$ and finally for $z \gtrsim 27$, the $2s$ states are totally emptied, recovering the no-node sequence. To see the reason for this, we should note that the depth of V_{core} is nearly proportional to z. Therefore as z is increased, the centrifugal potential, which is independent of z, becomes relatively unimportant compared with V_{core} in Eq. (1), bringing $1s$, $2p$, $3d$, etc. states closer in energy.

A similar crossover of configurations takes place by variation of R_c. Figure 4 shows the R_c dependence of the total energy for the lowest-energy three configurations ($1s^2 2p^6 3d^{10} 2s^2$, $1s^2 2p^6 3d^{10} 1s^1 4f^1$, and $1s^2 2p^6$-

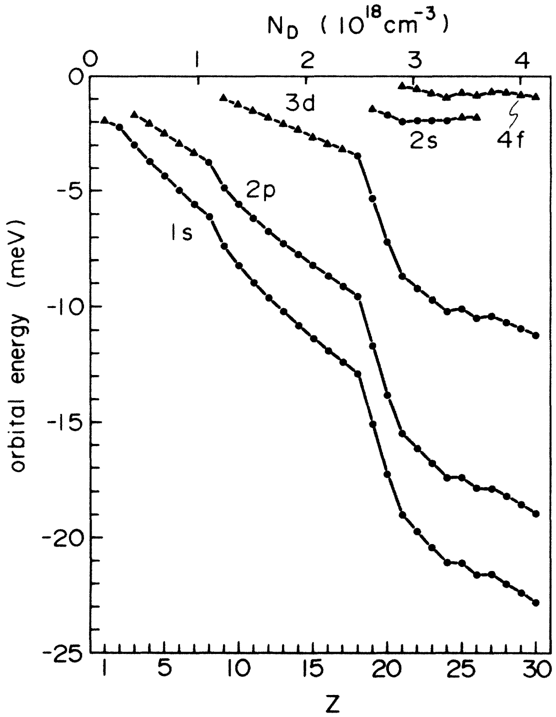

FIG. 3. Calculated orbital energies of the $Al_{0.35}Ga_{0.65}As$-GaAs superatom ($z=20$, $R_c=120$ Å) as a function of z. The triangles and dots denote partly occupied and fully occupied electron shells, respectively. Note that the donor concentration N_d is well below the solubility limit ($\sim 10^{19}$ cm^{-3}).

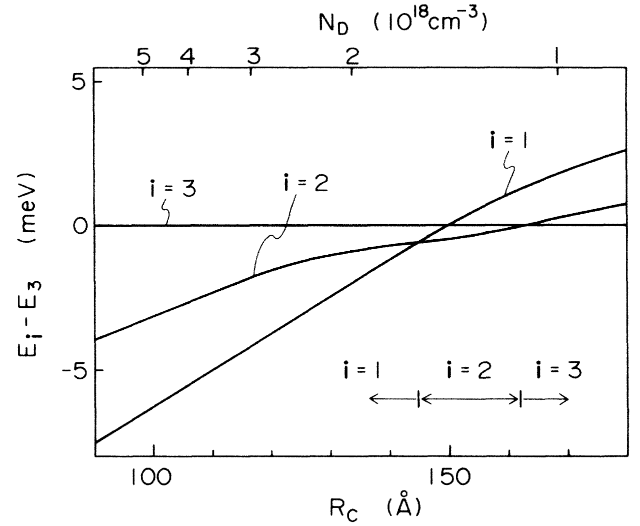

FIG. 4. R_c dependence of the calculated total energies E_i of the $Al_{0.35}Ga_{0.65}As$-GaAs superatom ($z=20$, $R_c=120$ Å) for different configurations i (N_d denotes donor concentration). Configurations considered are $1s^2 2p^6 3d^{10} 2s^2$ (denoted as $i=1$), $1s^2 2p^6 3d^{10} 2s^1 4f^1$ ($i=2$), and $1s^2 2p^6 3d^{10} 4f^2$ ($i=3$). For convenience, $E_i - E_3$ is plotted instead of E_i. The ground-state configurations are indicated in the lower part.

$3d^{10}4f^2$) in case of $z=20$. For $R_c < 145$ Å, the $2s^2$ configuration is the ground state, but as R_c is increased and hence the potential depth is reduced, the $4f$ states come down in energy and finally for $R_c > 162$ Å the $4f^2$ configuration becomes the ground state.

The excitation energy for the ground state, i.e., the energy difference between the ground and the first excited configurations, is on the order of millielectronvolts, except in the vicinity of a configuration crossover such as occurs around $R_c = 150$ Å for $z=20$. Thus the ground state is thermally stable at moderately low temperatures on the order of 1 K.

If we increase m^* for the matrix, the kinetic energy and the centrifugal energy terms in Eq. (1) are reduced while the potential energy is much less affected (only V_{xc} is affected by m^*). Therefore we get deeper bound states and a smaller superatomic radius. A reduction in ε brings about a similar change in the electronic structure. This, however, is due to the deepening of the potential. Both of these changes in the parameters tend to bring down the no-node states in the energy level sequence. For example, if, in the above superatom with $z=20$ and $R_c=120$ Å, we multiply m^* by 10 (i.e., $m^* = 0.67m_0$), the resulting ground-state configuration is $1s^2 2p^6 3d^{10} 4f^2$ and the binding energies in millielectronvolts are 15.07 ($1s$), 14.47 ($2p$), 13.39 ($3d$), and 11.83 ($4f$). Also, by replacing ε by $\varepsilon/2$ (i.e., $\varepsilon = 6.45$), we again get $1s^2 2p^6 3d^{10} 4f^2$ for the ground state, with binding energies 27.78 ($1s$), 23.75 ($2p$), 15.56 ($3d$), and 4.20 ($4f$) meV. The electronic structure depends rather strongly on R_c. However, even for small R_c, the outermost orbital remains shallow because of the small m^* and large ε of GaAs. (If $z=1$, the model tends, as $R_c \rightarrow 0$, to that of the hydrogenic donor.)

TABLE I. Electron occupation numbers for the $2s$ and $4f$ shells in Fig. 3.

z	$2s$	$4f$	z	$2s$	$4f$
19	1	0	26	1	7
20	2	0	27	0	9
21	2	1	28	0	10
22	2	2	29	0	11
23	2	3	30	0	12
24	2	4	31	0	13
25	1	6	32	0	14

As we have seen, superatoms are fascinating especially when combined to form molecules or crystals. A salient feature of such systems is the large freedom in the choice of the structure—both symmetry and inter(super)atomic distance. Also, because such a system exhibits no structural relaxation, degenerate ground states could be stable since Jahn-Teller[12] or Peierls[13] instabilities are irrelevant. Another interesting thing to note is the possible appearance of large-l states ($4f$, $5g$, $6h$, etc.), which may give rise to unique magnetic properties. Finally, by arrangement of superatoms in a perfectly periodic fashion it is possible to form a "superatom metal" with large r_s. Such a system will be an ideal tool to test various properties of a low-density electron gas such as free-electron ferromagnetism[14] and Wigner crystallization.[15]

In summary, we have clarified the general features of the electronic structure of the superatom through a self-consistent local-density-functional calculation. We believe that superatom physics will evolve into an important field where physics and technology go hand in hand.

We acknowledge valuable discussions with H. Watanabe and N. Hamada.

---

[1] B. Schwarzschild, Phys. Today **39**, 17 (1986).

[2] *The Physics and Fabrication of Microstructures and Microdevices,* edited by M. J. Kelly and C. Weisbuch (Springer-Verlag, Heidelberg, 1986).

[3] H. Watanabe, in Ref. 2, p. 5.

[4] H. Watanabe and T. Inoshita, Optoelectron. Dev. Technol. **1**, 33 (1986).

[5] See, for example, L. D. Landau and E. M. Lifshitz, *Quantum Mechanics* (Pergamon, Oxford, 1977), Chap. 10.

[6] The effective-mass approximation (EMA) should be quite valid for a sufficiently large core in view of its success in AlGaAs-GaAs single heterostructures. EMA becomes questionable as the core size is reduced, and the lower limit for the core diameter is estimated to be 30 Å. This is based on the fact that the electronic structure of $(\mathrm{GaAs})_n(\mathrm{AlAs})_n$ superlattices is well described by Kronig-Penney model, a drastically simplified version of EMA, down to $n=10$ (AlAs layer thickness ~30 Å) [A. Ishibashi, Y. Mori, M. Itabashi, and N. Watanabe, J. Appl. Phys. **58**, 2691 (1985)]. In the present paper, we treat cases where the core is much larger than this.

[7] J. Perdew and A. Zunger, Phys. Rev. B **23**, 5048 (1981).

[8] D. M. Ceperley and B. J. Alder, Phys. Rev. Lett. **45**, 566 (1980).

[9] While the Ceperley-Alder potential (Ref. 8, Appendix C) is based on the Hamiltonian $H=-\sum\Delta_i/2+\sum 1/|\mathbf{r}_i-\mathbf{r}_j|$, we need the exchange-correlation potential for the effective mass Hamiltonian $H'=-\sum\Delta_i/(2m^*)+\sum 1/|\mathbf{r}_i-\mathbf{r}_j|\varepsilon$. If we note that H' is obtained by replacing $\mathbf{r}_i$ in H by $(m^*/\varepsilon)\mathbf{r}_i$ and multiplying H by m^*/ε^2, we arrive at the relation given in the text.

[10] F. Stern and S. das Sarma, Phys. Rev. B **30**, 840 (1984).

[11] W. D. Knight, K. Klemenger, W. A. de Heer, W. A. Saunders, M. Y. Chou, and M. L. Cohen, Phys. Rev. Lett. **52**, 2141 (1984); Y. Ishii, S. Ohnishi, and S. Sugano, Phys. Rev. B **33**, 5271 (1986).

[12] See, for example, Ref. 5, p. 407.

[13] R. Peierls, *Quantum Theory of Solids* (Clarendon, Oxford, 1955), p. 108.

[14] K. A. Brueckner and K. Sawada, Phys. Rev. **112**, 328 (1958).

[15] E. P. Wigner, Phys. Rev. **46**, 1002 (1934).